Exploring Independent Effects of Follicle-Stimulating Hormone *In Vivo* in a Mouse Model

Yanjing Guo[1,2,3], **Wei Li**[2,3], **Yinghan Wang**[2]

[1] The Affiliated Hospital of Qingdao University [2] Department of Anesthesiology, Shandong Provincial Hospital Affiliated to Shandong First Medical University [3] Department of Anesthesiology, Shandong Provincial Hospital, Cheeloo College of Medicine, Shandong University

Corresponding Author

Yanjing Guo

guoyanjing@sdfmu.edu.cn

Abstract

During the transition from a reproductive to a nonreproductive phase (menopause), many women experience significant physiological and pathological changes, including decreased bone mass, increased blood lipids, and increased visceral adiposity. Levels of follicle-stimulating hormone (FSH) rise during the menopausal transition. Many studies have shown that FSH in various extragonadal tissues and organs is associated with the pathogenesis of multiple diseases. Thus, building an animal model that can help study the independent effects of FSH *in vivo* is particularly important. In this study, C57BL/6 female mice were ovariectomized and supplemented with estradiol valerate (OVX + E2) to eliminate the effect of the hypothalamic-pituitary-gonadal axis. The OVX + E2 mice received solvent (N.S.) or different doses of recombinant FSH via intraperitoneal injection to create a mouse model (OVF) characterized by relatively stable estrogen and rising FSH levels. Thus, we successfully generated an experimental mouse model to mimic the early stage of menopause transition, characterized by elevated serum FSH levels. The OVF model has the advantages of being stable, low cost, and easy to operate, which is suitable for studies to explore the extragonadal actions of FSH. Here, we describe detailed protocols for the mouse OVF model.

Introduction

Levels of follicle-stimulating hormone (FSH) rise during the menopausal transition (the term menopausal transition was defined in 2011 at stages of reproductive aging workshop (STRAW) + 10 system)[1]. It is during the menopausal transition, a period characterized by rising FSH levels and relatively stable estrogen[1], thatwomen experience menstrual cycle changes and significant physiological changes involving various cells and tissues. These changes can seriously affect the quality of life and health of women. Exploring the effects of FSH may improve women's quality of life and health.

FSH is secreted from gonadotrope cells in the anterior pituitary and is critical in controlling gonadal function and

reproduction[2]. The function of FSH is mediated through the FSH receptor (FSHR), which belongs to the G protein-coupled receptor (GPCR)[3]. FSHR is generally expressed in gonads, namely, the ovary and testis. It has been proved that FSHR is universally expressed in multiple extragonadal cells and tissues, including liver[4], hippocampus[5], osteoclasts[6], adipocytes[7], and endothelial cells[8]. Emerging studies have revealed extra gonadal actions of FSH and its potential clinical relevance in dyslipidemia[4], Alzheimer's disease[5], osteoporosis[9,10], atherosclerosis[11], obesity[9], and cancer[12]. Thus, building an animal model that can help study the independent effects of FSH *in vivo* is particularly important in exploring the actions of FSH alone.

In the protocol, we introduced the procedure for establishing a mouse model with relatively stable estrogen and rising FSH levels[13]. The mouse model mimics the menopause transition by ovariectomized surgery and then supplemented with estradiol valerate and recombinant FSH. As the ovariectomized mice were supplemented with exogenous estrogen to maintain similar estrogen levels with the sham-operated mice, the levels of endogenous FSH were stable due to estrogen feedback at the pituitary gland. In this condition, it could control the FSH levels by administering exogenous FSH without altering the estrogen levels. Thus, the OVF mouse model can exclude the influence of estrogen and observe the extragonadal physiological and pathological effects of FSH. We believe the detailed and visualized procedure is useful for researchers to establish the OVF mouse model in their laboratory and apply it to investigate physiological and pathological changes during the menopause transition as needed.

Protocol

The following protocol complied with all institutional ethical guidelines regarding the use of research animals and was approved by the Animal Ethics Committee at Shandong Provincial Hospital, China. All surgical manipulations were performed under deep anesthesia, and the animals did not experience pain at any stage during the procedure.

1. Pre-operation preparation

1. Instrument sterilization

   1. Steam-sterilize surgical instruments in an autoclave (121°C for 15 min) prior to the surgery. Prepare sufficient disposable sutures and needles.

2. Surgery platform setup

   1. Perform the surgery in a room dedicated to surgical procedures. Assign a bench area of at least 60 cm x 60 cm for the operation. Clean the surface of the area with 75% alcohol and cover with a disposable medical towel, and then disinfect it with ultraviolet radiation 30 min in advance (**Figure 1A**).

3. Animal preparation

   1. House all animals in a temperature-controlled room (20-25 °C) with a 12 h light, 12 h dark cycle. Acclimate 8-week-old female C57BL/6 mice to the housing facility for 1 week before surgery.

   2. Weigh mice before the surgery. Administer all 9-week-old female mice with general anesthesia by intraperitoneal injection of Tribromoethanol (280 mg/kg), to achieve painlessness at any stage during the procedure. Inject meloxicam (2 mg/kg)

subcutaneously, about 1 h before an operation to relieve pain.

3. Apply eye ointment to prevent corneal dryness during the surgery.

4. Apply hair removal lotion on the back using a clean cotton swab. Let the lotion sit on a mouse for 3-5 min, then remove the hair using gauze and cotton swabs. Repeat this step until all hair has been removed from the back of the mouse.

5. Use gauze and cotton swabs to clean the skin with 75% alcohol. Fix the mouse on the surgery platform back up using a rubber strip or cotton rope (**Figure 1B**) and apply iodophor solution to clean the back.
NOTE: Confirm the depth of anesthesia via a toe-pinch before Ovariectomy.

2. Ovariectomy

NOTE: Tribromoethanol can be maintained for approximately 30 min, ensuring the surgery is completed as much as possible.

1. Make a ~1.0 cm dorsal incision longitudinally from the thigh base upwards using a disposable scalpel, ensuring that only the skin and subcutaneous fascia are incised and avoiding cutting into the posterior peritoneum at this time.

2. Pull the incision to the left, and a white fat pad can be seen. Cut ~0.5 cm along the white fat pad to expose the intraperitoneal cavity using micro-forceps and scissors.

3. After cutting the posterior peritoneum, slowly and gently remove the white fat pad from the intraperitoneal cavity with micro-forceps. Immediately moisten the white fat tissue with 0.9% sterile saline outside the soaked gauze.

Keep exposed tissue always moistened while outside the abdominal cavity.

4. A pink granular substance, namely the ovary, is attached to the lower part of the white fat pad (**Figure 2A**). The ovaries are connected to a slender duct, namely the uterus. Use 5-0 absorbable sutures to ligate the ovarian end of the uterus and remove the left ovary (**Figure 2B**).

5. When removing an ovary, preserve the surrounding fatty tissue as much as possible. Avoid direct contact between surgical instruments and the ovaries and prevent intraperitoneal implantation of ovarian tissue.

6. Carefully place the white fat pad back in the intraperitoneal cavity. Perform a simple intermittent suture on the posterior peritoneum with a 5-0 absorbable suture (**Figure 2C**). After the suture is complete, clean any bleeding with 0.9% sterile saline-soaked gauze.

7. Pull the skin incision to the right and remove the right ovary using the same method.

8. Perform an intermittent suture with 4-0 non-absorbable sutures and clean any bleeding with 0.9% sterile saline-soaked gauze (**Figure 2D**).

9. Clean the wound with an iodophor solution after completing both sutures. Intraperitoneally inject broad-spectrum antibiotics.

3. Post-operation observation

1. Move the mice to a 37 °C constant temperature blanket after the surgery. Until the mice can move freely, keep the animals in their individual cage. Do not leave the animal unattended until it has regained sufficient consciousness to maintain sternal recumbency.

2. Inject meloxicam (2 mg/kg) subcutaneously 24 h after the operation to relieve pain.

3. Monitor the mice daily to ensure that the surgical wound is healing properly without any signs of complications (dehiscence) present.

4. Estradiol supplementation

1. Prepare feed supplemented with estradiol valerate. Use 2.6 mg beta-estradiol 17-valerate supplemented per 1 kg of feed.

2. At 3 days after the completion of the surgery, feed the mice with estradiol valerate.

5. FSH injection

1. Prepare recombinant human FSH solution. Dissolve recombinant human FSH powder for injection with 0.9% sterile saline to 100 IU/mL.

2. Group mice according to experimental plans and give solvent or different doses of recombinant FSH via intraperitoneal injection for 2 weeks. According to the biological activity of recombinant FSH, use the injection dose of FSH in mice equivalent to the serum FSH level in women during the menopausal transition period.
   NOTE: Based on different treatments, ovariectomized estrogen-supplemented mice were randomly divided into three groups, solvent (N.S.) group receiving 100 µL/day solvent, low-dose FSH (L-FSH) group receiving 15 IU/kg body weight per day and high-dose FSH (H-FSH) group receiving 30 IU/kg body weight per day.

Representative Results

The OVF mouse model mimics the early stage of menopause transition with relatively stable estrogen and rising FSH levels[13]. First, for ovary removal surgery, 9-week-old female C57BL/6 mice were administered general anesthesia and subjected to either a sham operation (Sham) or bilateral ovariectomy (OVX). As smear images of Papanicolaou stained cells clearly identified the proestrus, estrus, metestrus, and diestrus stages of the estrous cycle, the OVX mice lost the estrous cycle (**Figure 3A**), and the ELISA method showed a significant decrease in serum estradiol (E2) levels (**Figure 3B**). Second, the OVX mice were supplemented with beta-estradiol 17-valerate (OVX + E2) to maintain serum estrogen at the same level as the Sham group. Third, the OVX + E2 mice received solvent (N.S.) or different doses of recombinant FSH via intraperitoneal injection to create a mouse model (OVF) characterized by relatively stable estrogen and rising FSH levels (**Figure 4**).
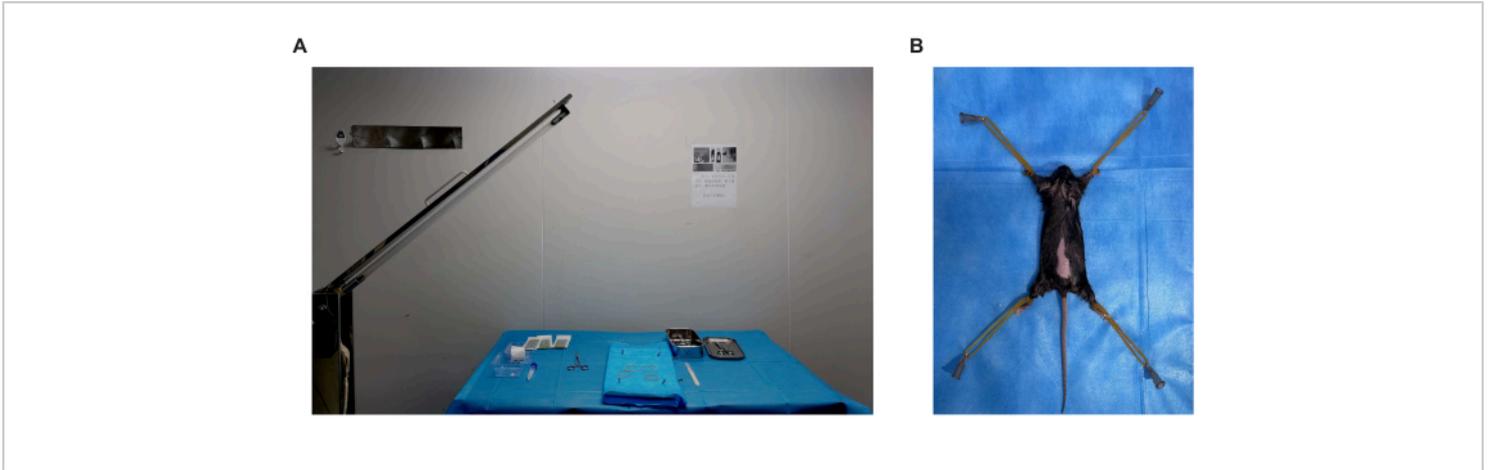
Figure 1. Surgical environment and mouse posture. (**A**) A bench area of at least 60 cm x 60 cm for the operation. Clean the surface of the area with 75% alcohol and cover it with a disposable medical towel, and then disinfect with ultraviolet radiation 30 min in advance. (**B**) Fix the mouse on the surgery platform back up using a rubber strip or cotton rope.
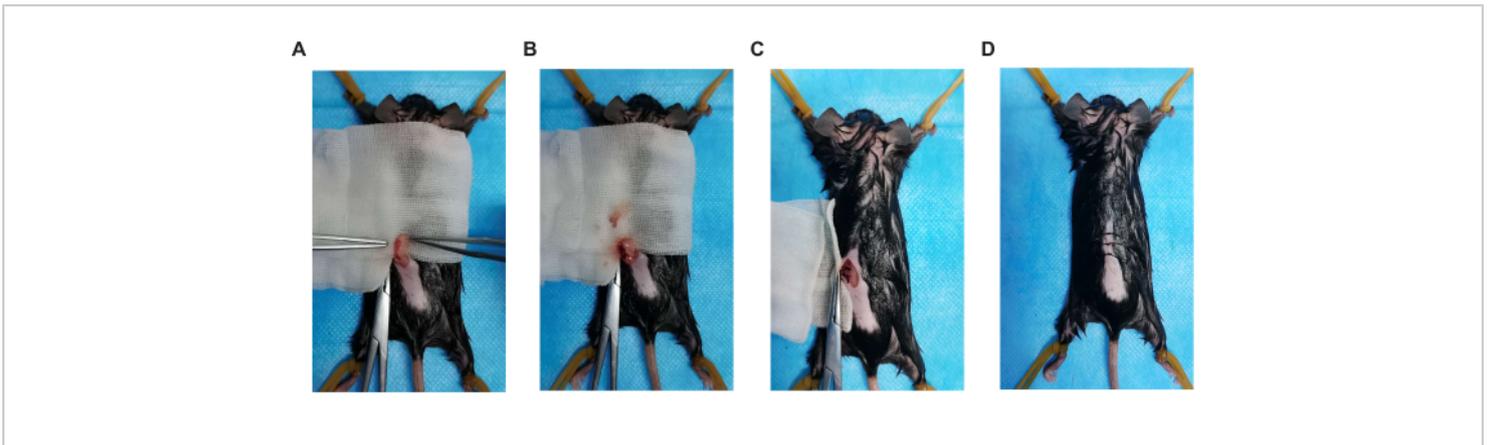

Figure 2. Key steps of surgical operation. (**A**) Ovarian position, (**B**) ovariectomy, (**C**) suture peritoneum, and (**D**) suture skin incision.
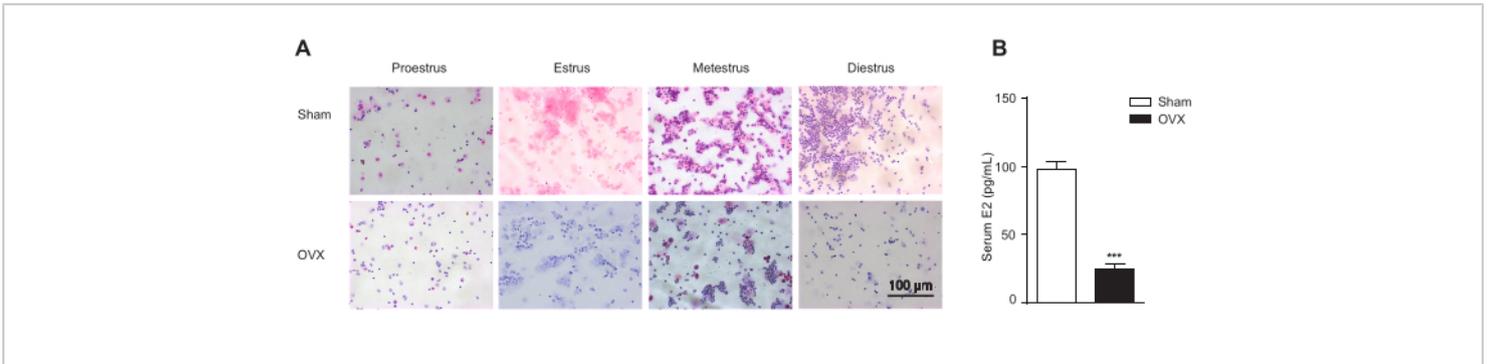
Figure 3. Vaginal cytology. Vaginal cytology represents stages of the estrous cycle and endogenous estrogen in the ovariectomized mice (OVX) and the sham-operated ones (Sham; n = 12 for the Sham group; n = 10 per OVX groups). (**A**) Vaginal cytology represents stages of the estrous cycle according to the relative presence of leukocytes, cornified epithelial cells, and nucleated epithelial cells. Stages of the estrous include proestrus, the predominance of nucleated epithelial cells; estrus, the predominance of enucleated cornified cells; metestrus, the presence of leukocytes, and cornified and nucleated epithelial cells; diestrus, the predominance of leucocytes. Scale bar = 100 μm. (**B**) Endogenous estrogen in the ovariectomized mice (OVX) and the sham-operated ones (Sham). Data are shown as the mean ± SEM. Student's t-test is used for statistical analysis. ***$p < 0.001$. Please click here to view a larger version of this figure.
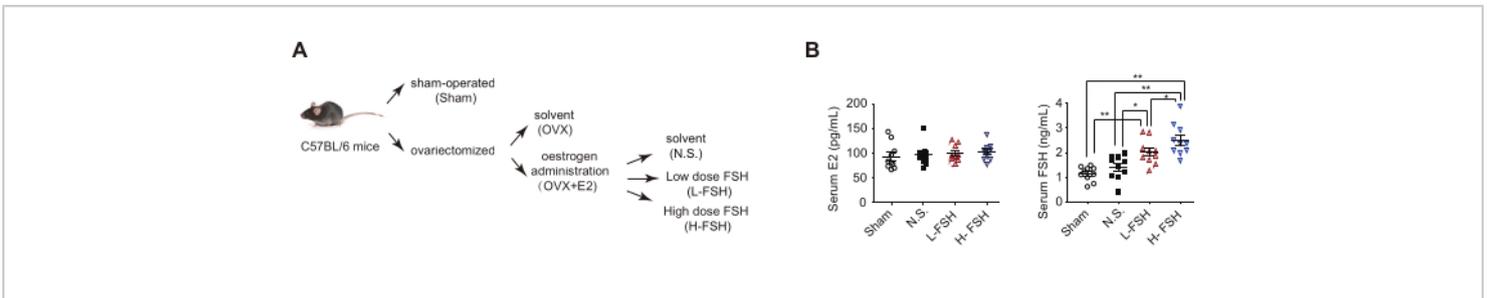

Figure 4. OVF model and serum hormone levels. (**A**) Flow-chart OVF model. (**B**) ELISA analysis of serum estrogen (E2) and FSH concentrations. Data are represented as the mean ± SEM. One-way ANOVA was used for statistical analysis. * $p < 0.05$ and ** $p < 0.01$. This figure has been modified from[4]. Please click here to view a larger version of this figure.

Discussion

During the transition from a reproductive to a nonreproductive phase (menopause), many women experience significant physiological and pathological changes. Levels of FSH rise during the menopausal transition[1]. Emerging studies have revealed that FSH in various extragonadal tissues and organs is critical in the pathogenesis of multiple diseases, including dyslipidemia[4], Alzheimer's disease[5], osteoporosis[9,10], atherosclerosis[11], obesity[9], and cancer[12]. Thus, building an animal model that can help study the independent effects of FSH *in vivo* is particularly important. The OVF mouse model mimics the early stage of menopause

transition with relatively stable estrogen and rising FSH levels and is particularly suitable for studies to explore the extragonadal actions of FSH.

In this method, ovariectomy was made using a single dorsal back incision, approximately 1 cm from the thigh base upwards (**Figure 1B**). The skin was cut almost together with the dorsal muscles using sharp dissecting scissors, and the peritoneal cavity was thus accessed. After the operation, the muscle incision required no suturing, and the skin wound was closed bilaterally with one catgut suture (**Figure 2**). The operation is technically easier, less time-consuming, and less harmful for female mice as compared to other methods used.

Some details that should be attended to during the surgery procedure. First, all surgical procedures should be kept clean and as sterile as possible to reduce the risk of postoperative infection. Second, because the ovarian tissue is very fragile, surgical instruments cannot contact the ovaries directly during ovariectomy, to avoid intraperitoneal implantation. Third, after the surgery, the mice were moved to a 37 °C constant temperature blanket during recovery to prevent postoperative hypothermia leading to death.

A previous study has proved that endogenous estrogen is synthesized in the ovarian theca cells of premenopausal women or adipose stromal cells of the breast of postmenopausal women and in minor quantities in peripheral tissue[14]. The serum estrogen dropped sharply for ovariectomized mice but cannot be eliminated (**Figure 3B**). However, endogenous estrogen synthesized in extragonadal tissue does not affect the stability of estrogen levels in the OVF model (**Figure 4B**).

There are some limitations in the OVF model. Once the surgical operation is not careful and leads to ovarian intraperitoneal implantation, it may lead to model failure. In this case, the serum estrogen does not drop sharply and fluctuates during different stages of the estrous cycle. After exogenous administration of estrogen and FSH, it takes approximately 1 week for the body to reach equilibrium. Thus, pathological changes of the OVF model that occur within 1week cannot indicate the effects of FSH.

In conclusion, the OVF model has the advantages of being stable, low-cost, and easy to operate. The systemic effects of high-level FSH can be observed after intraperitoneal injection of FSH; that is, the OVF model is suitable for studies that explore the extragonadal actions of FSH. However, requirements for model surgery and intraperitoneal injection procedures are quite high. If funding is sufficient, specific knockout models are the best choice.

Disclosures

The authors have nothing to disclose.

Acknowledgments

References

1. Harlow, S. D. et al. Executive summary of the Stages of Reproductive Aging Workshop + 10: addressing the unfinished agenda of staging reproductive aging. *Journal of Clinical Endocrinology & Metabolism.* **97** (4), 1159-1168 (2012).

2. Ulloa-Aguirre, A., Zariñán, T. The Follitropin Receptor: Matching Structure and Function. *Molecular Pharmacology.* **90** (5), 596-608 (2016).

3. Franks, S., Stark, J., Hardy, K. Follicle dynamics and anovulation in polycystic ovary syndrome. *Human Reproduction Update.* **14** (4), 367-378 (2008).

4. Guo, Y. et al. Blocking FSH inhibits hepatic cholesterol biosynthesis and reduces serum cholesterol. *Cell Research.* **29** (2), 151-166 (2019).

5. Xiong, J. et al. FSH blockade improves cognition in mice with Alzheimer's disease. *Nature.* **603** (7901), 470-476 (2022).

6. Sun, L. et al. FSH Directly Regulates Bone Mass. *Cell.* **125** (2), 247-260 (2006).

7. Liu, X. M. et al. FSH regulates fat accumulation and redistribution in aging through the Gαi/Ca(2+)/CREB pathway. *Aging Cell.* **14** (3), 409-420 (2015).

8. Maclellan, R. A. et al. Expression of Follicle-Stimulating Hormone Receptor in Vascular Anomalies. *Plastic and Reconstructive Surgery.* **133** (3), 344e-351en (2014).

9. Liu, P. et al. Blocking FSH induces thermogenic adipose tissue and reduces body fat. *Nature.* **546** (7656), 107-112 (2017).

10. Ji, Y. et al. Epitope-specific monoclonal antibodies to FSHβ increase bone mass. *Proceedings of the National Academy of Sciences of the United States of America.* **115** (9), 2192-2197 (2018).

11. El Khoudary, S. R. et al. Trajectories of estradiol and follicle-stimulating hormone over the menopause transition and early markers of atherosclerosis after menopause. *European Journal of Preventive Cardiology.* **23** (7), 694-703 (2016).

12. Radu, A. et al. Expression of Follicle-Stimulating Hormone Receptor in Tumor Blood Vessels. *The New England Journal of Medicine.* **363** (17), 1621-1630 (2010).

13. Sowers, M. R. et al. Endogenous hormones and bone turnover markers in pre- and perimenopausal women: SWAN. *Osteoporosis International.* **14** (3), 191-197 (2003).

14. Kristensen, V. N., Kure, E. H., Erikstein, B., Harada, N., Børresen-Dale, A.L. Genetic susceptibility and environmental estrogen-like compounds. *Mutation Research/Fundamental and Molecular Mechanisms of Mutagenesis.* **482** (1), 77-82 (2001).